




## Original Article

# MINIMALLY MANIPULATED AUTOLOGOUS CELL THERAPY FOR PRESSURE INJURY MANAGEMENT IN SPINAL CORD INJURY: AN *IN VITRO* SEMINAL STUDY

A. Bertolo<sup>1,2,\*</sup> , S. Sonntag<sup>1</sup>, N. Nyfeler<sup>1</sup>, S. Satkunaseelan<sup>1</sup>, J. Buergin<sup>3</sup>, A. Haumer<sup>3</sup>, N. Speck<sup>3</sup>, R. Wettstein<sup>1,3</sup>  and J. Stoyanov<sup>1,2</sup> 

<sup>1</sup>SCI Population Biobanking & Translational Research Group, Swiss Paraplegic Research, 6207 Nottwil, Switzerland

<sup>2</sup>Institute of Social and Preventive Medicine, University of Bern, 3012 Bern, Switzerland

<sup>3</sup>Department of Plastic, Reconstructive, Aesthetic and Hand Surgery, University Hospital of Basel, 4051 Basel, Switzerland

## Abstract

**Background:** Pressure injuries (PIs) remain a formidable challenge in patients with spinal cord injury (SCI) due to their reduced regenerative capacity. This study established an *in vitro* platform for a minimally manipulated autologous cell-based approach that integrated adipose-derived stromal cells (ADSCs), platelet-rich plasma (PRP), and collagen scaffolds to accelerate the healing of PIs. **Methods:** ADSCs were isolated through mechanical processing of lipoaspirates, yielding distinct fat fractions—namely “Microfat”, “emulsified Microfat”, and “Nanofat”—which were subsequently characterised via flow cytometry and trilineage differentiation assays. Three-dimensional ADSC constructs using various collagen scaffolds were assessed for their ability to support adipogenic differentiation of ADSCs. The influence of PRP at different concentrations was evaluated on ADSCs proliferation, cellular senescence, and in co-culture with human umbilical vein endothelial cells (HUVECs). Additionally, the impact of ADSCs-derived exosomes on stemness maintenance was investigated. **Results:** Quantitative analyses demonstrated that “emulsified Microfat” enhanced ADSC delivery and reduced cellular senescence. Cell constructs using stiffer scaffolds demonstrated improved adipogenic differentiation. Supplementation with 5 % PRP effectively promoted ADSC proliferation and supported ADSC-HUVEC co-culture, showing results comparable to standard growth factor conditions in cultures. Although exosome treatment did not modify ADSCs proliferation rates, it was associated with an increased expression of stem cell markers. **Conclusions:** Altogether, these findings provide a preclinical foundational framework for future regenerative treatment strategies aimed at improving tissue repair following surgical intervention for PIs in patients with SCI.

**Keywords:** Pressure injuries, spinal cord injury, adipose-derived stromal cells, adipogenesis, platelet-rich plasma, wound healing.

**\*Address for correspondence:** A. Bertolo, SCI Population Biobanking & Translational Research Group, Swiss Paraplegic Research, 6207 Nottwil, Switzerland; Institute of Social and Preventive Medicine, University of Bern, 3012 Bern, Switzerland. Email: [alessandro.bertolo@paraplegie.ch](mailto:alessandro.bertolo@paraplegie.ch).

**Copyright policy:** © 2025 The Author(s). Published by Forum Multimedia Publishing, LLC. This article is distributed in accordance with Creative Commons Attribution Licence (<http://creativecommons.org/licenses/by/4.0/>).

## Introduction

Pressure injuries (PIs), also known as pressure ulcers or bedsores, are chronic wounds that arise from prolonged pressure on the skin and underlying tissues. Their pathogenesis is multifactorial, involving external contributors such as shear forces, friction, and moisture, as well as internal factors, including malnutrition, anaemia, and endothelial dysfunction [1]. PIs significantly reduce patients' quality of life and may become life-threatening, particularly in individuals with limited mobility. Patients with spinal cord injury (SCI) are at an elevated risk of developing PIs due to impaired mobility, absent protective sensory perception, and compromised healing capacity of the denervated

skin [2]. Epidemiological data from two studies conducted at the Swiss Paraplegic Centre in 2013 and 2022 reported that approximately 50 % of hospitalised patients with SCI developed PIs during their primary rehabilitation period [3,4]. PIs are the second most common cause of unplanned hospital readmission in this population, following urinary tract complications, and they impose a significant burden on healthcare systems because of the need for surgical intervention and extended inpatient care [5]. The chronic and slow-healing nature of PIs increases the risk of both short- and long-term complications, including bacteraemia, osteomyelitis, squamous cell carcinoma, and sinus tract formation [6]. Current treatment strategies for PIs in patients with SCI are resource-intensive, often necessitating surgi-

cal reconstruction and prolonged hospitalisation, and are frequently complicated by delayed healing, infection, and high recurrence rates [7]. These limitations have raised interest in regenerative approaches aimed at promoting more effective and durable wound healing. Cell-based therapies and tissue engineering techniques offer promising alternatives to conventional treatments by restoring the structural integrity and functional competence of damaged tissues. These strategies have the potential to reduce scar formation, accelerate healing, and generate more resilient tissue that is less prone to injury recurrence [8]. Recent advances have underscored the therapeutic potential of adipose-derived stromal cells (ADSCs) in enhancing the healing of chronic wounds.

ADSCs, a subset of mesenchymal stem cells (MSCs), possess remarkable self-renewal capacity and multipotent differentiation potential, making them promising candidates for PIs treatment. These precursor cells can differentiate into key lineages involved in skin regeneration, including fibroblasts, keratinocytes, and endothelial cells [9], as well as loose connective tissue [10]. In addition to their differentiation capabilities, ADSCs secrete a diverse array of bioactive molecules, such as pro-regenerative growth factors, anti-inflammatory cytokines, pro-angiogenic mediators, and wound-healing peptides, which collectively support and enhance the tissue repair process [11]. ADSCs also play a pivotal role in promoting angiogenesis, which is a critical component of wound healing. They contribute to neovascularization by differentiating into vascular endothelial cells and supporting the formation of capillary-like structures [12]. Fat grafts are a naturally rich source of ADSCs, providing both cellular and extracellular matrix components.

Fat grafts offer practical advantages, including ease of harvest, favourable safety profile, cost-effectiveness, and biocompatibility [13]. Fat grafting is an autologous and homologous tissue transfer procedure in which adipose tissue is harvested and reinjected during the same procedure. Fat has many attributes of an ideal material: it is available in sufficient quantities, naturally integrates into host tissues, and may offer long-term durability. Clinically, fat grafting has become a standardised and widely accepted method for soft tissue augmentation and regenerative applications, including facial volume restoration, enhancement of skin elasticity, and mitigation of photoaging-related damage [14]. Early techniques have been refined to obtain long-term survival with grafted fat [15], for example, based on an injectable product obtained by emulsification, filtration of the lipoaspirate, and mechanical fragmentation [16]. This technique involves processing aspirated adipose tissue via microcutting using a Nanocube device (Lipocube, London, UK), resulting in injectable products enriched with extracellular matrix components, ADSCs, and stromal cells. The regenerative potential of processed fat grafts can be further improved by incorporating bioactive agents such as

platelet-rich plasma (PRP) and ADSC-derived exosomes and embedding these cells within biocompatible scaffolds.

Platelet-rich plasma (PRP) is prepared by sequential centrifugation of anticoagulated autologous blood, resulting in a concentrated plasma fraction enriched with platelet-derived alpha granules. These granules contain a diverse pool of growth factors critical for tissue repair and regeneration, including platelet-derived growth factor (PDGF), vascular endothelial growth factor (VEGF), transforming growth factor- $\beta$  (TGF- $\beta$ ), insulin-like growth factor (IGF), and epidermal growth factor (EGF) [17]. When applied independently, autologous PRP has demonstrated regenerative efficacy and the ability to accelerate wound healing [18], with optimal clinical effects observed at platelet concentrations exceeding one million platelets per microliter [19]. In addition to its growth factor content, the fibrin matrix formed in PRP functions as a provisional biological scaffold, promoting MSCs survival and retention while reducing apoptosis in adipocytes [20]. Furthermore, a meta-analysis of 34 clinical trials involving 2458 patients showed that MSCs and platelet-rich plasma significantly accelerated wound healing, enhanced vascularization, reduced pain, and lowered recurrence rates [21]. PRP also exhibits anti-inflammatory effects, which contribute to the reduction of fat necrosis and cellular apoptosis, further supporting its clinical utility in adipose tissue regeneration and potential application in the treatment of PIs [13].

Similarly, exosome-based therapies represent an innovative approach to modulating ADSCs function and promoting ulcer healing outcomes [22]. Exosomes are nanoscale extracellular vesicles secreted by stem cells and other cell types, containing a diverse cargo of bioactive molecules, including proteins, lipids, and various RNA species, which mediate intercellular communication [23]. These vesicles facilitate the targeted delivery of regenerative signals, offering a cell-free therapeutic approach that retains the anti-inflammatory, immunomodulatory, and regenerative properties of their parent cells, including ADSCs [24]. ADSC-derived exosomes have been shown to promote angiogenesis during wound healing [25] and stimulate dermal fibroblasts to produce collagen types I and III and elastin [26]. These effects contribute to improved cutaneous wound repair and reduced scar formation [27]. In addition to the benefits of using exosomes, the incorporation of ADSCs into biocompatible scaffolds further enhances tissue regeneration by supporting cell localisation, maintaining differentiation potential, and providing structural stability, which is particularly important for load-bearing anatomical sites. Collagen scaffolds, in particular, offer a three-dimensional (3D) porous architecture that facilitates ADSC activity and allows for the controlled, sustained release of exosomes, thereby prolonging their therapeutic impact [28]. Collagen-based biomaterials have been widely applied in tissue engineering for applications such as ligament repair [29], cartilage regeneration [30], and dermal

grafting [31], underscoring their clinical versatility and relevance. Collectively, the integration of ADSCs, PRP, exosomes, and supportive scaffolds has the potential to constitute a multifaceted regenerative strategy capable of enhancing tissue integration, stimulating neovascularization, and accelerating wound healing.

In this study, we adopted a translational approach that combined complementary components, including ADSCs, PRP, biocompatible scaffolds, and exosome-based therapies, into a comprehensive treatment strategy for PIs. By harnessing the synergistic potential of these components, we aimed to establish a robust *in vitro* foundation to inform future regenerative strategies and improve healing outcomes in patients with PIs.

## Material & Methods

### Donor Population

This study was conducted in accordance with the Declaration of Helsinki [32]. All six male patients who provided biological samples (mean age  $51 \pm 5$  years) had traumatic SCI. The eligibility criteria included a diagnosis of SCI and the presence of severe PIs (grades III and IV). All recruited patients underwent fasciocutaneous flap reconstruction for PIs at the Swiss Paraplegic Centre in Nottwil, Switzerland, between June 2020 and September 2022.

### Adipose-Derived Mesenchymal Stromal Cell Isolation

Adipose tissue was processed using the Lipocube Nano System (Lipocube Nano Kit, Cat #901890840019; Lipocube, London, UK) to generate various fat particle sizes. Unprocessed lipoaspirate, termed “Millifat”, was filtered through the Lipocube to obtain “Microfat” (fat particle size under 1.2 mm). The Microfat was then emulsified by passing it ten times through the Lipocube system and subsequently refined into “Nanofat” (fat particles between 0.4–0.6 mm) via an additional filtration step [33]. Finely minced adipose tissue and liposuction-derived samples were digested with 0.075 % collagenase type II (355 U/mg, Cat #17101-015, lot #371087; Worthington, Lakewood, NJ, USA) for 60–90 minutes at 37 °C, as described previously [34]. Following digestion, the mixture was centrifuged at 700 g for 10 minutes at room temperature (RT) to separate and discard the lipid-rich layer. The cell pellet was washed once with phosphate-buffered saline (PBS) and red blood cells were lysed by incubating the pellet for 2 minutes at RT in a solution containing 0.15 M ammonium chloride (Cat #A3661, lot #6L004172), 1 mM potassium hydrogen carbonate (Cat #A2375, lot #3J001518) (both AppliChem, Darmstadt, Germany), and 0.1 mM ethylenediaminetetraacetic acid (EDTA) (Cat #A1104, lot #GL006070; AppliChem, Darmstadt, Germany). The resulting cells were resuspended in minimum essential medium, Eagle’s  $\alpha$  modification ( $\alpha$ -MEM) (Cat #1-23S50-I, lot #TJ0472P; Bioconcept, Allschwil, Switzerland) supplemented with 10 % foetal bovine serum (FBS) (#10500-064, Cat #10438-

26, lot #2372691RP; Gibco, Waltham, MA, USA), and  $1 \times$  penicillin-streptomycin solution (Cat #15140-122, lot #1910856; Gibco). Cells were cultured at 37 °C in a humidified atmosphere with 5 % CO<sub>2</sub>. To stimulate proliferation, cells were seeded at a density of  $2 \times 10^3$  cells/cm<sup>2</sup> and cultured in a medium containing 5 ng/mL fibroblast growth factor (FGF) (Cat #100-18B, lot # 021308; Peprotech, Waltham, MA, USA) until they reached sub-confluence. Only ADSCs from passages 1 to 4 were used in subsequent experiments. At each passage, the cells were counted, and their volume was assessed using a Scepter Cell Counter (Version 2.0, Cat #PHCC20040; Merck, Buchs, Switzerland). All cells were cryopreserved at –150 °C. ADSCs were analysed using the MycoAlert® PLUS Mycoplasma Detection Kit (LT07-701, lot #0073223056; Lonza, Basel, Switzerland) and found to be mycoplasma-free.

### Phenotypic Characterization of ADSCs

Following expansion, ADSCs were characterised by flow cytometry. Approximately  $10^5$  cells per tube were incubated for 30 minutes at room temperature in PBS containing a 1:50 dilution of the following antibodies: cluster of differentiation (CD)14-fluorescein isothiocyanate (FITC) (NB100-77759, lot #B1537727; Novus Biological distributed by LubioScience, Zürich, Switzerland), CD44-FITC (NBP1-41278, lot #516653; Novus Biological), CD90-FITC (NBP1-96125, lot #52837; Novus Biological), and CD105-FITC (MCA1557A488T, lot #0710; Novus Biological). After incubation, cells were washed and resuspended in PBS. Fluorescence was measured using a CytoFLEX flow cytometer (Model No. A00-1-1102; Beckman Coulter Life Sciences, Nyon, Switzerland), and data were analysed using FlowJo v.10.0 software (Treestar, Ashland, OR, USA).

### Senescence Detection Assay

Cellular senescence was assessed using an autofluorescence-based method [35]. ADSCs (at P1) were pre-treated with 100 nM bafilomycin A1 (Sigma-Aldrich, Merck, Darmstadt, Germany) for 1 hour to inhibit lysosomal acidification. Cells were detached with pre-warmed 0.05 % trypsin-EDTA, resuspended in PBS containing the viability stain TO-PRO-3 (Cat #R37170, lot #1928338; Molecular Probes, Waltham, MA, USA) and incubated for 15 minutes. Autofluorescence was measured using a 488 nm excitation laser and a 525/50 nm detection filter, while TO-PRO-3 fluorescence was measured with a 638 nm laser and 670/30 nm detection filter. To standardise settings between runs, 15  $\mu$ m polypropylene calibration beads (Cat #PHCCBEADS, lot #114218900; Merck, Darmstadt, Germany) were used (5000 events per run), and dead cells were excluded from the analysis. Data were analysed using FlowJo software.

**Table 1. Human genes used for quantitative RT-PCR.**

Gene (NCBI reference sequence)	Primer nucleotide sequence (5' to 3')	Amplicon length (bp)
Housekeeping gene		
<i>β-actin</i> (NM_002046)	F-CCAACCGCGAGAAGATGA	97
	R-CCAGAGGCGTACAGGGATAG	
<i>GAPDH</i> (NM_001101)	F-GGAAGCTTGTCATCAATGGAA	102
	R-TGGACTCCAGGACGTACTCA	
Adipogenic markers		
<i>FABP4</i> (NM_001442)	F-TGTAGGTACCTGGAAACTTGTC	199
	R-AAATTCCTGGCCCAGTATGAAG	
<i>GLUT4</i> (NM_001042)	F-GGCATGGGTTTCAGGTACTCTT	117
	R-GCCTCGAGTTTCAGGTACTCTT	
<i>LPL</i> (NM_000237)	F-ACACAGCTGAGGACACTTGC	227
	R-CACTGGGTAATGCTCCTGAG	
Endothelial markers		
<i>CD31/PECAM-1</i> (NM_000442)	F-TCCCCTAAGAATTGCTGCCA	151
	R-TTCTTCCCAACACGCCAATG	
<i>vWF</i> (NM_000552)	F-CTGTGCTATGTCATGCCAC	193
	R-TCCATCCTCACCAATGCACT	
<i>VEGFR2</i> (NM_002253)	F-CGCATCACATCCACTGGTATT	76
	R-TTGTCACTGAGACAGCTTGG	
Stem cell markers		
<i>CD90</i> (NM_006288)	F-AGGACGAGGGCACCTACAC	107
	R-GCCCTCACACTTGACCAGTT	
<i>MCP-1/CCL2</i> (NM_002982)	F-TCAAACCTGAAGCTCGCACTCT	129
	R-GTGACTGGGGCATTGATTG	

F, forward; R, reverse; bp, base pairs; *vWF*, von Willebrand factor; *FABP4*, fatty acid binding protein 4; *GLUT4*, glucose transporter type 4; *LPL*, lipoprotein lipase; *GAPDH*, glyceraldehyde 3-phosphate dehydrogenase; *CD31*, cluster of differentiation 31; *VEGFR2*, vascular endothelial growth factor receptor 2; RT-PCR, real time polymerase chain reaction; NCBI, National Center for Biotechnology Information.

### Platelet Rich Plasma and Exosome Preparations

PRP was isolated from the patients' blood using sequential centrifugation. Initially, blood was centrifuged at 150 g for 10 minutes at 4 °C in monovettes. The plasma layer was transferred to a new tube and centrifuged again at the same parameters. The platelet-rich plasma fraction, located in the bottom layer, was then concentrated by centrifugation at 800 g for 15 minutes at 4 °C. The final PRP preparation was stored at –20 °C for short-term or –80 °C for long-term preservation. Activation of PRP was achieved through a series of freeze-thaw cycles: aliquots were thawed at 37 °C, vortexed briefly, frozen on dry ice for 15 minutes, and then thawed and vortexed again, followed by centrifugation at 2000 g for 10 minutes at 4 °C. The supernatant was pooled, diluted with PBS to a concentration ten times that of the starting plasma, and filtered using a 0.2 µm filter (Cat #SFM33PE0022S, lot #I2A49035; cobetter, Hangzhou, China). Autologous PRP was then mixed with culture medium at concentrations of 1 %, 3 %, 5 %, and 10 % for experimental use.

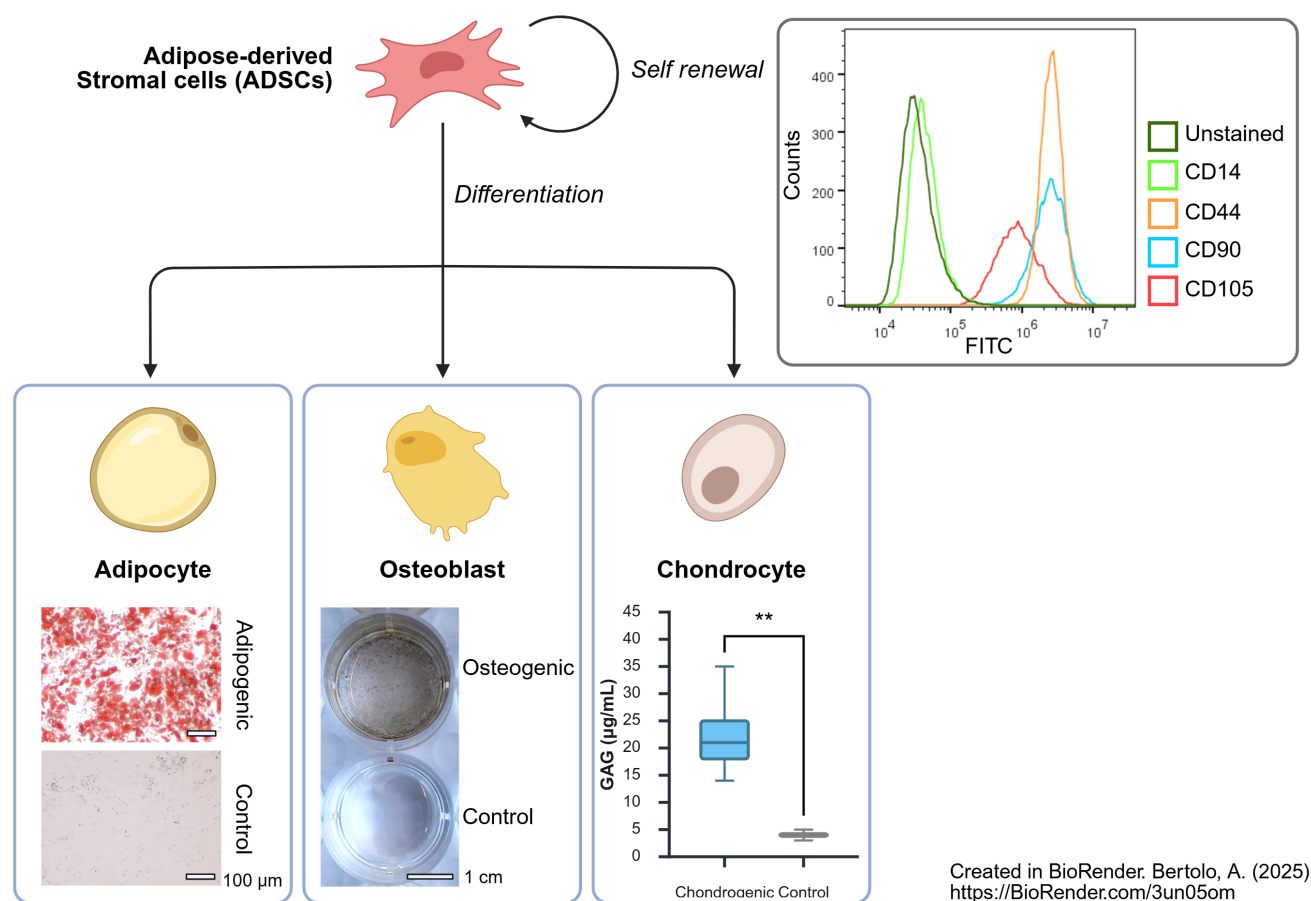
Exosome preparations were obtained from a commercially available skincare solution (ASCE Dermal Signal Kit; ExoCoBio, Seoul, Republic of Korea) [36,37].

Lyophilised exosomes were resuspended in 0.02 µm-filtered PBS to achieve a final concentration of 10 mg/mL (equivalent to 10<sup>9</sup> exosomes/mL). These exosomes were derived from ADSCs obtained from healthy donors and isolated using a tangential flow filtration-based method optimised for large-scale production, ensuring both high yield and purity [38]. While autologous exosomes offer ideal immunological compatibility, standardised, commercially available exosome preparations present several practical advantages for clinical and experimental applications. These include consistent quality control, extensive safety testing, and reduced donor-to-donor variability, all of which can be influenced by age, sex, and overall health status [39].

### RNA Isolation, Complementary DNA (cDNA) Synthesis and Real Time Polymerase Chain Reaction (PCR)

Total RNA was extracted from monolayer cultures using Direct-zol RNA MiniPrep kit (Cat #R2060, lot #256174; Zymo, LucernaChem, Luzern, Switzerland). For three-dimensional cell constructs, homogenisation was performed using a Dispomix device (Cat #130-093-237, lot #5150901432; Axonlab, Baden, Switzerland) and Aurum Total Mini Kit (Cat #7326820; lot #64562842; Bio-Rad





Created in BioRender. Bertolo, A. (2025)  
<https://BioRender.com/3un05om>

**Fig. 1. Characterization of ADSCs by surface marker expression and multipotent differentiation potential.** The upper right panel displays flow cytometry data confirming that ADSCs express the mesenchymal markers *CD44*, *CD90*, and *CD105*, but lack the haematopoietic marker *CD14*. The lower panels illustrate the differentiation capacity of ADSCs: the bottom left panel shows Oil Red O staining of lipid vacuoles following adipogenic induction (scale bar = 100 µm); the bottom middle panel shows mineral deposition detected by Von Kossa staining following osteogenic differentiation (scale bar = 1 cm); and the bottom right panel quantifies glycosaminoglycan (GAG) production in µg/mL following chondrogenic differentiation, with Alcian blue staining as a marker. Negative controls for each differentiation test were included for comparison. \*\*Statistical significance ( $p < 0.01$ ); ADSCs, adipose-derived stromal cells; FITC, fluorescein isothiocyanate; *CD14*, cluster of differentiation 14. Created in BioRender. Bertolo, A. (2025) <https://BioRender.com/3un05om>.

Laboratories, Basel, Switzerland), following the manufacturer's instructions. For each sample, 500 ng of RNA was reverse transcribed to cDNA using the VILO cDNA Synthesis Kit (Cat #11754-250, lot #2331350; Invitrogen, Waltham, MA, USA). The cDNA was subsequently diluted 1:10 with ultrapure water prior to use. Real-time PCR reactions were prepared using the primers listed in Table 1 (250 nM), 5 µL of cDNA template, and 1× IQ SYBR Green Supermix (Cat #1708882, lot #64505532; Bio-Rad) in a total volume of 20 µL, performed in 96-well plates. The PCR protocol comprised an initial denaturation at 95 °C for 3 minutes, followed by 35 cycles of 95 °C for 15 seconds, 60 °C for 20 seconds, and 72 °C for 20 seconds. Melting curve analysis was performed post-amplification, and relative gene expression was calculated using the  $2^{-\Delta\Delta C_t}$  method, normalising to  $\beta$ -actin and glyceraldehyde 3-phosphate dehydrogenase (*GAPDH*) [40].

### 3D Cell Construct Preparation for Adipogenic Assay

Collagen pads, approved for use as wound dressings for soft tissue regeneration, were aseptically cut into 3 mm cubes from three collagen sources: equine collagen (Cat #A901698718, lot #2MCL15; BioPad, Euroresearch, Milan, Italy), pure unmodified heterologous collagen (Cat #02188120, lot #421111811; Suprasorb C, Lohmann & Rauscher, St. Gallen, Switzerland), and cross-linked porcine collagen (Cat #400141; lot #82000191; Geistlich Fibro-Gide®, Geistlich, Wolhusen, Switzerland). Four cubes were prepared for each collagen type: three for gene expression analysis and one for immunohistochemical evaluation. ADSCs were suspended in PBS containing 2 % FBS and seeded onto the cubes at a density of  $1 \times 10^5$  cells per cube at various application sites. Following a 30-minute incubation at 37 °C to facilitate cell attachment, the

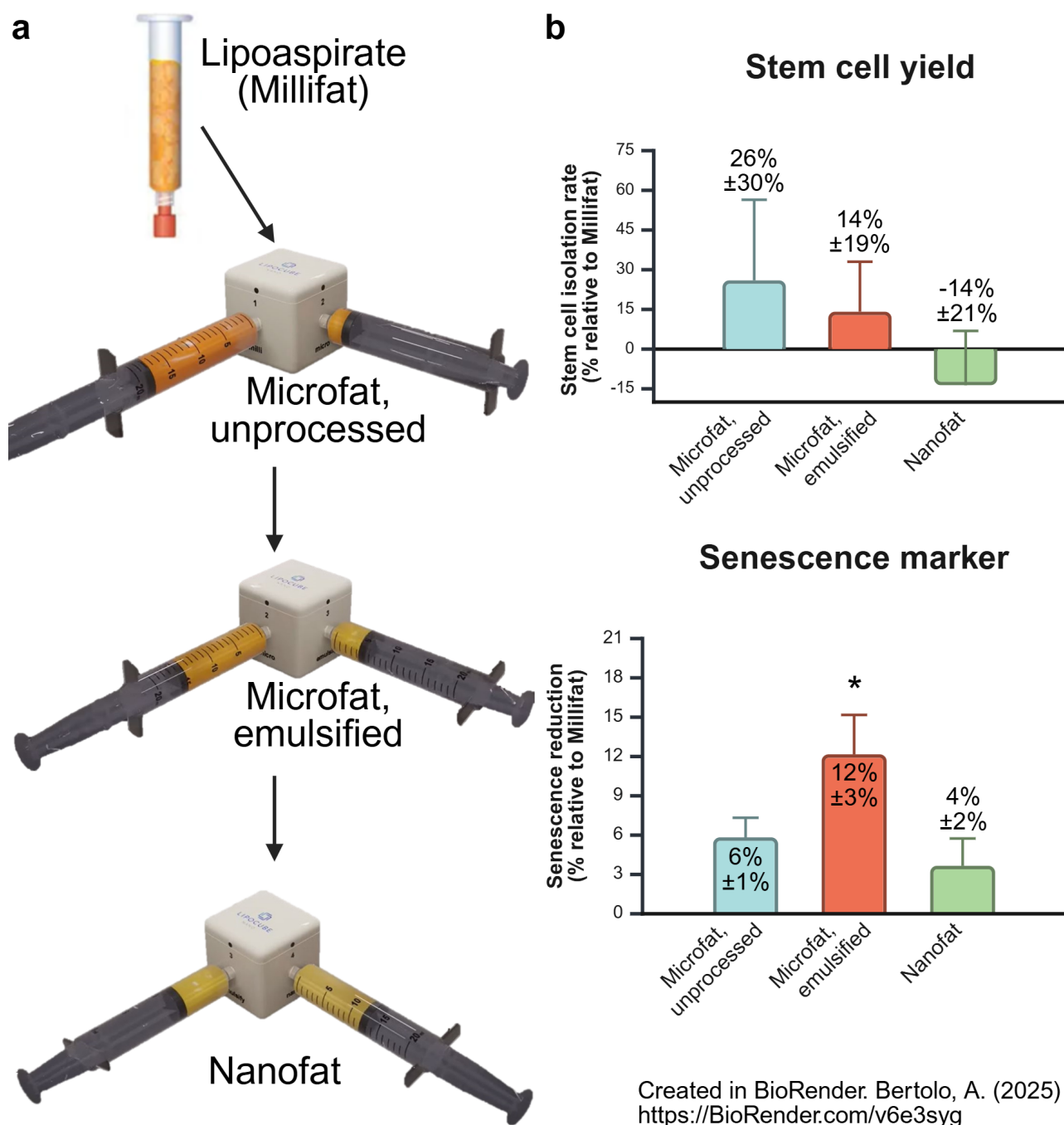
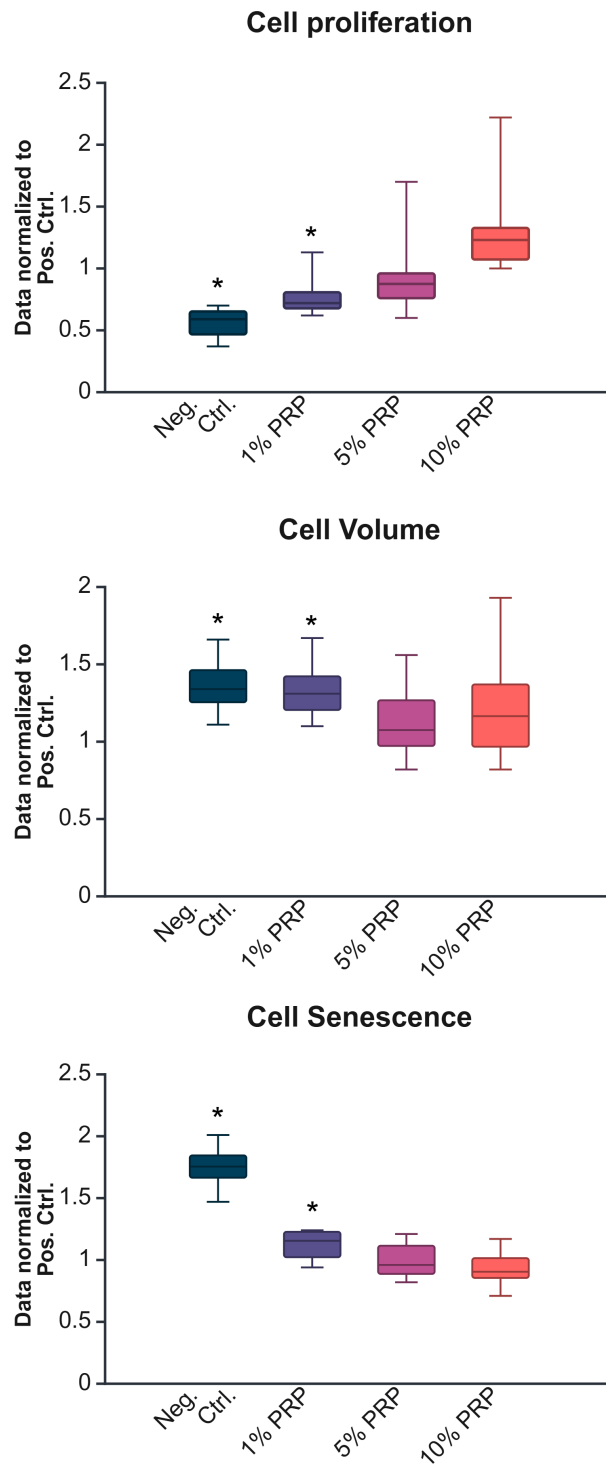


**Fig. 2. Effects of mechanical processing of lipoaspirates on stem cell yield and senescence.** (a) Schematic representation of the sequential mechanical processing of lipoaspirates using the Lipocube system, resulting in distinct adipose tissue fractions: unprocessed Microfat, emulsified Microfat, and Nanofat, derived from the original Millifat. (b) Bar graphs compare stem cell yield (top panel) and cellular senescence (bottom panel) across the different processing stages. Values were normalised to Millifat, the unprocessed control. Bars represent means and SEM,  $n = 6$ ; \*Statistical significance ( $p < 0.05$ ). SEM, standard error of the mean. Created in BioRender. Bertolo, A. (2025) <https://BioRender.com/v6e3syg>.

culture medium was gently added to each well. After two weeks of differentiation, the size of each cell construct was measured under a stereo binocular microscope.

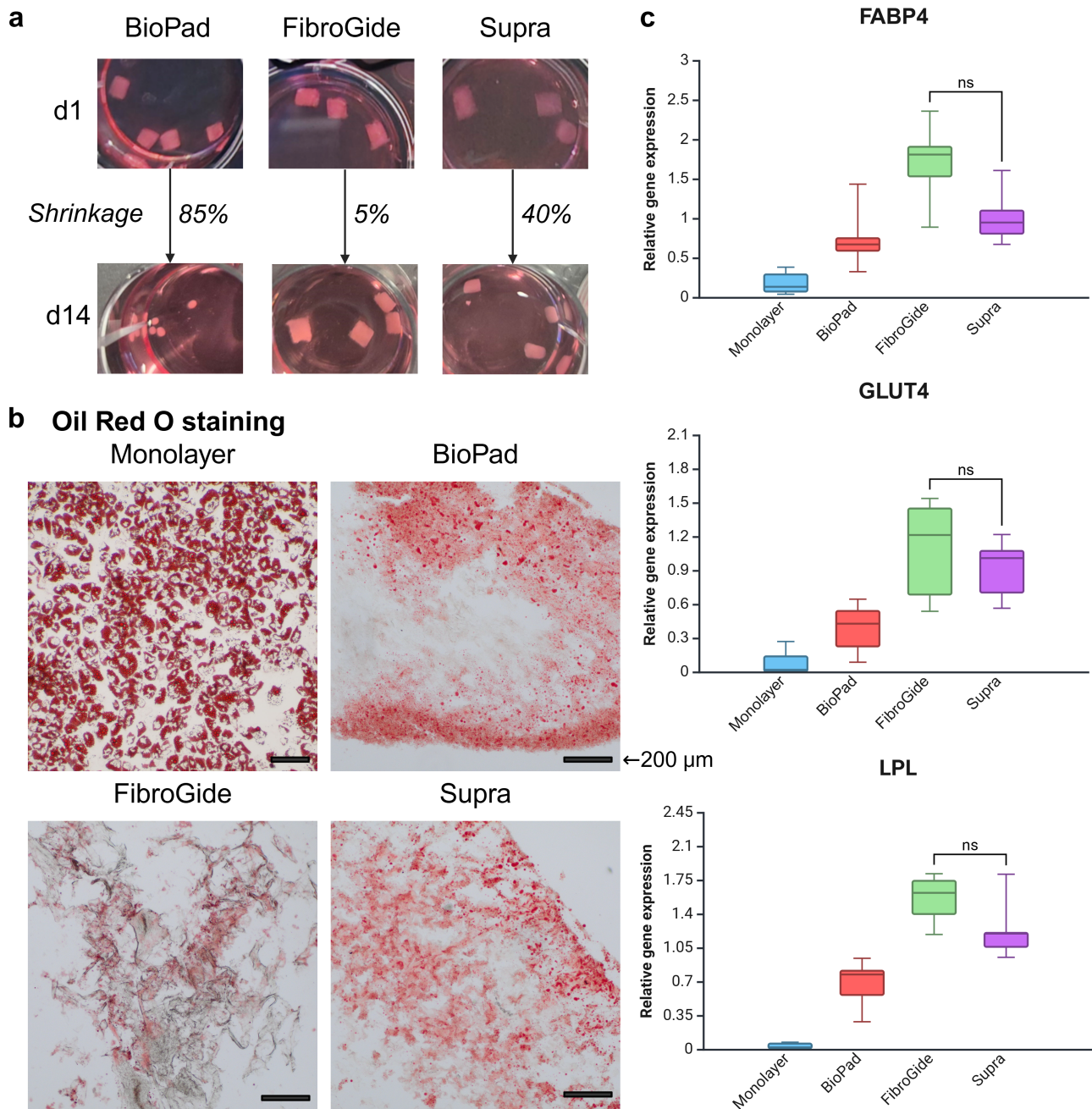
#### ADSCs and HUVEC Co-Culture in 3D, Cryosectioning and Staining

ADSCs and human umbilical vein endothelial cells (HUVEC, passage 2, C01510C, Gibco, Waltham, MA, USA) were co-cultured on Geistlich Fibro-Gide® (Fi-



Created in BioRender. Bertolo, A.  
(2025) <https://BioRender.com/lh0ehgl>

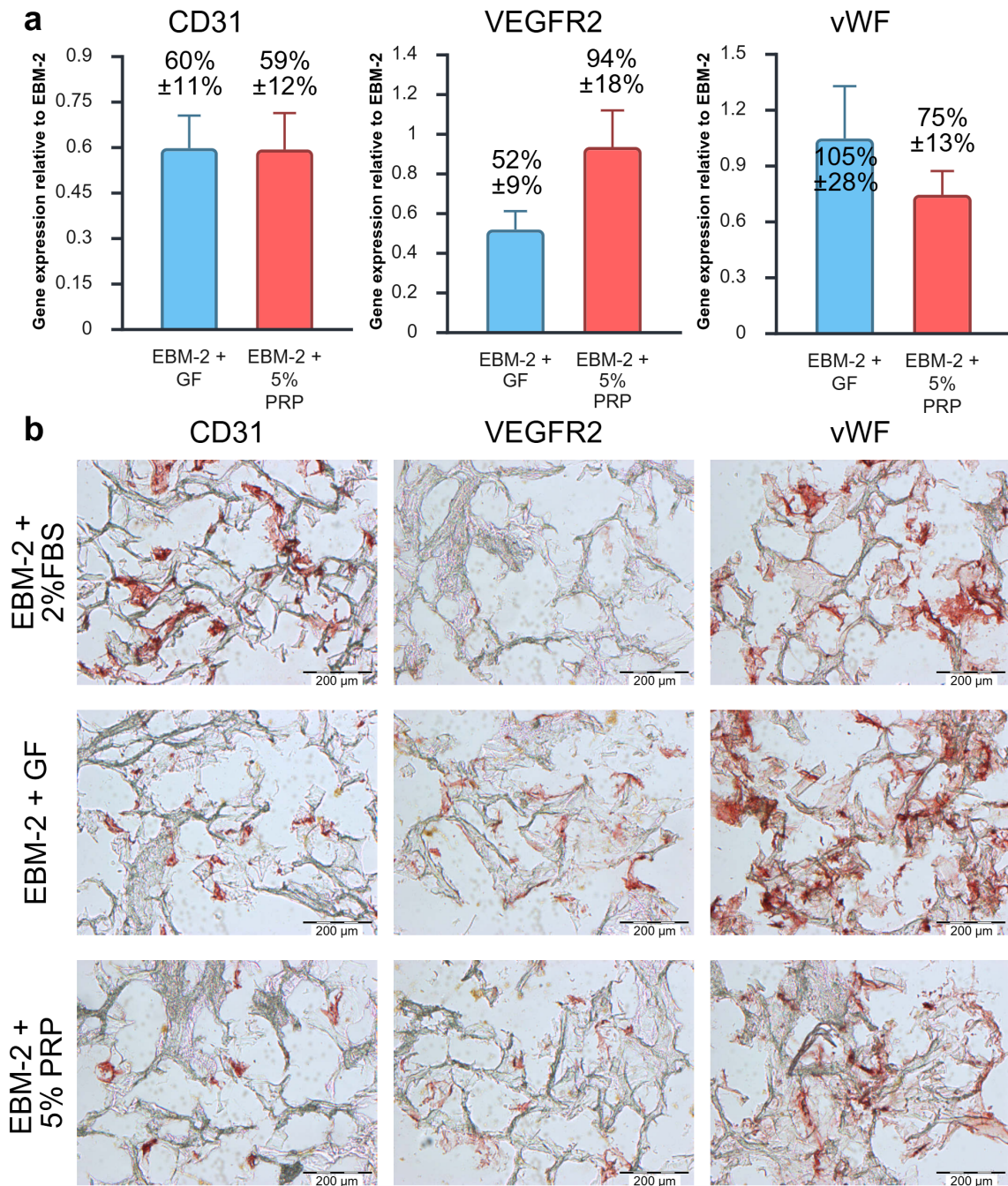
**Fig. 3. Effects of PRP on ADSCs cultured for 5 days.** Box plots display the impact of different PRP concentrations (1 %, 5 %, and 10 %) on cell proliferation (quantified by cell count, top panel), cell volume (measured in pL, middle panel), and cell senescence (assessed by fluorescence using a 488 nm excitation laser and a 525/50 nm emission filter, bottom panel). The experimental conditions were compared and normalised to the positive control (Pos. Ctrl.), in which cells were cultured in FGF-supplemented medium. In the negative control (Neg. Ctrl.), cells were maintained in FBS without FGF or PRP supplementation. Data were normalised to the positive control,  $n = 6$ ; \*Statistical significance compared to the positive control ( $p < 0.05$ ); PRP, platelet-rich plasma; FBS, foetal bovine serum; FGF, fibroblast growth factor. Created in BioRender. Bertolo, A. (2025) <https://BioRender.com/lh0ehgl>.



Created in BioRender. Bertolo, A. (2025) <https://BioRender.com/4zwvtz2>

**Fig. 4. Comparison of different scaffolds in supporting adipogenic differentiation of ADSCs.** (a) Representative images showing morphological changes and construct shrinkage in ADSCs cultured on three collagen-based scaffolds (BioPad, FibroGide, and Suprasorb) on day 1 (d1) and day 14 (d14); notably, constructs on BioPad exhibited significant shrinkage (approximately 85 %), whereas Suprasorb and FibroGide scaffolds showed moderate (40 %) and minimal (5 %) shrinkage, respectively. (b) Oil Red O staining demonstrated lipid droplet accumulation (in red), indicative of adipogenic differentiation in ADSCs cultured on each scaffold. Representative images of the monolayer controls and three scaffolds are shown. Scale bars = 200 μm. (c) Box plots display the relative gene expression levels of adipogenic markers *FABP4*, *GLUT4*, and *LPL* (n = 6) as assessed by qPCR (normalised to *β-actin* and *GAPDH*). Constructs cultured on FibroGide and Suprasorb scaffolds exhibited higher adipogenic marker expression than those on BioPad and monolayer controls. ns, no statistical significance; *FABP4*, fatty acid binding protein 4; *GLUT4*, glucose transporter type 4; *LPL*, lipoprotein lipase; *GAPDH*, glyceraldehyde 3-phosphate dehydrogenase; qPCR, quantitative polymerase chain reaction. Created in BioRender. Bertolo, A. (2025) <https://BioRender.com/4zwvtz2>.





Created in BioRender. Bertolo, A. (2025)  
<https://BioRender.com/5kie0pm>

**Fig. 5. Endothelial differentiation in co-cultures of ADSCs and HUVECs on FibroGide scaffolds.** (a) Relative gene expression levels of endothelial markers—*CD31*, *VEGFR2*, and von Willebrand factor (*vWF*)—in 3D co-cultures consisting of 80 % ADSCs and 20 % HUVECs. Two culture conditions were compared: EBM-2 medium supplemented with standard growth factors (EBM-2 + GF) and EBM-2 medium supplemented with 5 % PRP (EBM-2 + 5 % PRP). Expression levels were normalised to the baseline expression in cells cultured in EBM-2 medium + 2 % FBS, with data presented as means  $\pm$  SEM ( $n = 6$ ). (b) Representative immunohistochemical images illustrating the localisation of *CD31*, *VEGFR2*, and *vWF* within the 3D FibroGide constructs, confirming the presence of endothelial cells. Scale bars represent 200  $\mu$ m. HUVECs, human umbilical vein endothelial cells; 3D, three-dimensional; *VEGFR-2*, vascular endothelial growth factor receptor 2; EBM-2, endothelial basal medium-2; *CD31*, cluster of differentiation 31; GF, growth factors. Created in BioRender. Bertolo, A. (2025) <https://BioRender.com/5kie0pm>.

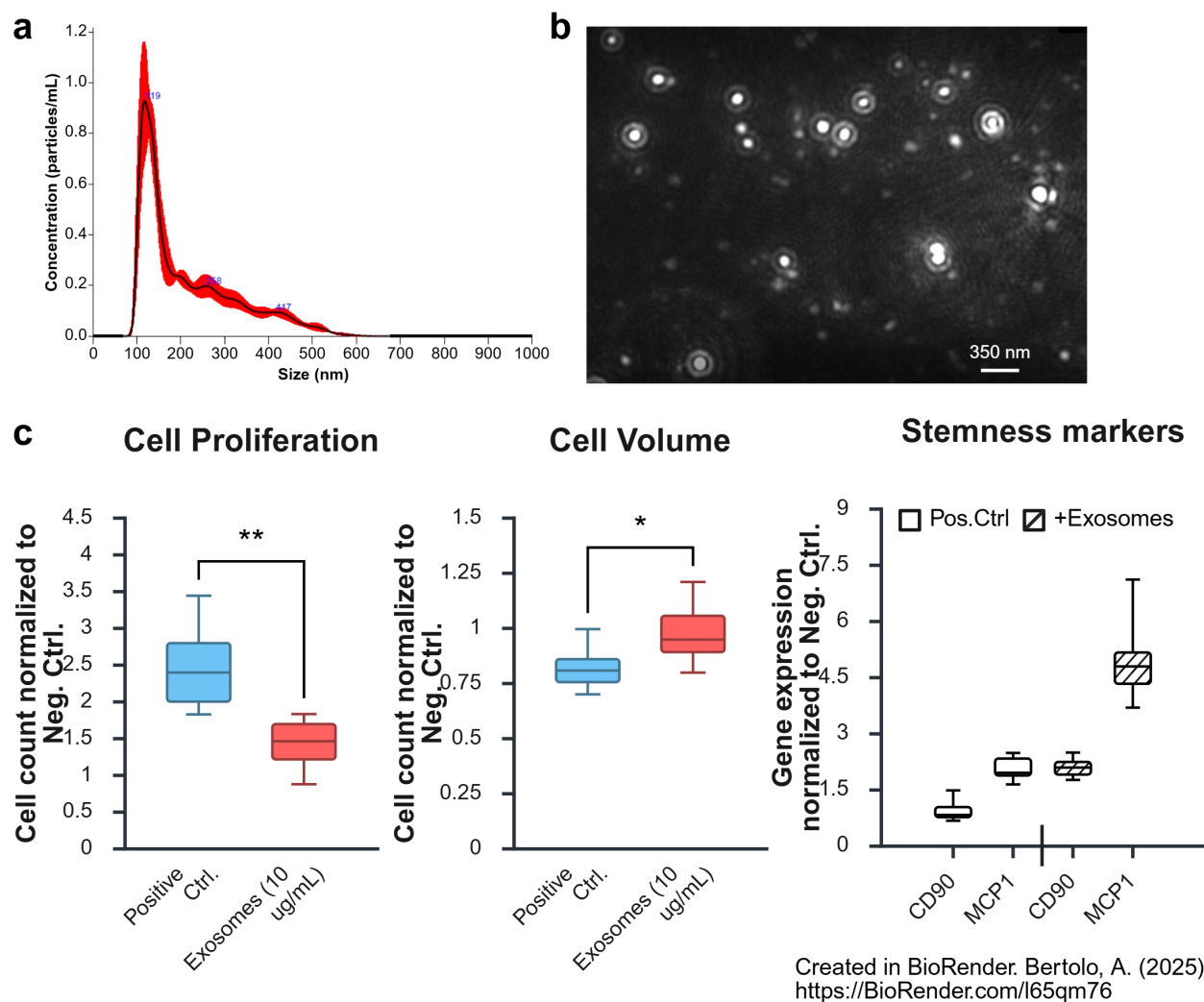


**Fig. 6. Characterisation of ADSC-derived exosomes and their effects on ADSCs cultured.** (a) Nanoparticle tracking analysis revealed the size distribution of exosomes, with the predominant particle size around 119 nm, illustrating particle concentration as a function of size (nm). (b) Representative fluorescence microscopy image of exosomes (scale bar = 350 nm). (c) Box plots display the impact of supplementing ADSCs cultures with 10 µg/mL exosomes on cell proliferation (cells/mL), cell volume (pL), and gene expression levels of *CD90* and *MCP-1*. All data were normalised to a negative control (cultures maintained without FGF supplementation). *n* = 6; \*Statistical significance ( $p < 0.05$ ); \*\*Statistical significance ( $p < 0.01$ ). Created in BioRender. Bertolo, A. (2025) <https://BioRender.com/l65qm76>.

broGide) scaffolds in endothelial basal medium-2 (EBM-2) basal medium (Cat #CC-3156, lot #0001006766; Lonza) supplemented with 2 % FBS. HUVEC were analysed using the MycoAlert® PLUS Mycoplasma Detection Kit and found to be mycoplasma-free. The medium was further supplemented with either 5 % PRP or a growth factor cocktail (endothelial cell growth medium (EGM)-2 medium containing hydrocortisone, FGF-2, VEGF, R3-insulin-like growth factor (IGF)-1, ascorbic acid, EGF, and sulphated gentamicin/amphotericin B; Cat #CC-4176, lot #00141; Lonza). The co-culture of ADSCs and HUVEC in an 8:2 ratio was incubated for 10 days. Post-culture, cell constructs were embedded in optimal cutting temperature (OCT) compound (Cat #361603E, lot #03831874; VWR Chemicals, Dietikon, Switzerland) for 30 minutes, frozen at  $-80^{\circ}\text{C}$ , and sectioned at 20 µm using a cryostat (Mi-

crom HM560, Histocom AG, Zug, Switzerland). For immunohistochemical analysis, endogenous peroxidases were quenched by incubating sections in 3 %  $\text{H}_2\text{O}_2$ /PBS at room temperature, followed by a PBS wash. Non-specific binding was blocked for 1 hour in PBS containing 1 mg/mL bovine serum albumin (BSA), 10 % FBS, and 0.1 % Triton X-100. Sections were then incubated overnight at  $4^{\circ}\text{C}$  with primary antibodies against *CD31* (mouse monoclonal, 1:50, BBA7, lot #k0907; R&D Systems, Minneapolis, MN, USA), *VEGFR2* (rabbit polyclonal, 1:50, BS-2089R, lot #P573; Bioss, Woburn, MA, USA), and von Willebrand factor (*vWF*) (rabbit polyclonal, 1:100, sc-14014, lot #D1409; Santa Cruz Biotechnology, Dallas, TX, USA) in blocking solution. After washing with PBS, sections were incubated for 2 hours with biotinylated secondary antibodies (goat anti-mouse, 1:200, B0529, Cat #A90-216P,

lot #A90-216P-21; goat anti-rabbit, 1:200, L42015, Cat #A120-201P, lot #A120-201p-10; both from Bethyl, Montgomery, AL, USA), followed by streptavidin-horseradish peroxidase (1:200, S2438, lot #109K6135; Sigma-Aldrich, Merck, Darmstadt, Germany) for 1 hour at RT. Visualisation was achieved using 0.075 % 3-amino-9-ethylcarbazole in a 0.01 %  $\text{H}_2\text{O}_2$  solution. The sections were mounted with 70 % glycerol (A3739, lot #2217823; AppliChem, Darmstadt, Germany) and examined under a light microscope (OLYMPUS IX71, Hamburg, Germany).

#### *ADSCs In Vitro Differentiation into Osteogenic, Chondrogenic and Adipogenic Lineages*

To confirm trilineage potential, ADSCs were induced to differentiate into osteogenic, chondrogenic, and adipogenic lineages. In all cases, the negative control consisted of ADSCs cultured in  $\alpha$ -MEM supplemented with 10 % FBS (#10500-064, Gibco, Waltham, MA, USA), 2.5  $\mu\text{g}/\text{mL}$  amphotericin B (A1907, lot #1T004206; AppliChem, Darmstadt, Germany), and 1 $\times$  penicillin-streptomycin solution (#15140-122, Gibco, Waltham, MA, USA).

#### Chondrogenic Differentiation

Collagen cubes (BioPad) were used as scaffolds to support the chondrogenic differentiation of ADSCs, as previously established as an appropriate scaffold for this application *in vitro* [41]. Cells ( $4 \times 10^5$  cells per cube) were seeded onto collagen cubes and allowed to adhere for 30 minutes before addition of the culture medium. The cell constructs were then cultured for three weeks at 5 %  $\text{O}_2$  in chondrogenic medium, which consisted of Advanced Dulbecco's Modified Eagle Medium (DMEM) + GlutaMAX (#11540446, lot #1775313; Gibco, Waltham, MA, USA), 2.5 % FBS, 1 $\times$  penicillin-streptomycin solution (#15140-122, Gibco, Waltham, MA, USA), 2.5  $\mu\text{g}/\text{mL}$  amphotericin B (A1907, AppliChem, Darmstadt, Germany), 40 ng/mL dexamethasone (D4902, lot #BCBL2140V; Sigma-Aldrich, Merck, Darmstadt, Germany), 50  $\mu\text{g}/\text{mL}$  ascorbic acid 2-phosphate (#49752, Cat #D4902, lot #SLBM7892V; Sigma-Aldrich, Merck, Darmstadt, Germany), 1 $\times$  Insulin-Transferrin-Selenium X (#12097549, lot #1724124; Gibco, Waltham, MA, USA), and 10 ng/mL transforming growth factor- $\beta$ 1 (TGF- $\beta$ 1, # 100-21, lot #0611209-1; Peprotech, Waltham, MA, USA).

Glycosaminoglycan (GAG) accumulation was quantified as a marker of chondrogenesis. After six hours of enzymatic digestion of the cell constructs at 60 °C using 125  $\mu\text{g}/\text{mL}$  papain (P4762, lot #5Y008189; Sigma-Aldrich, Merck, Darmstadt, Germany) in a buffer containing 5 mM L-cysteine-HCl (C1276, lot #1320377; Sigma-Aldrich, Merck, Darmstadt, Germany), 5 mM sodium citrate (#131655, lot #307596; AppliChem, Darmstadt, Germany), 150 mM NaCl (A2942, lot #76003985; AppliChem, Darmstadt, Germany), and 5 mM EDTA (A2937,

lot #2L011192; AppliChem, Darmstadt, Germany), GAG accumulation was measured using an Alcian blue binding assay [42]. Quantification was performed using chondroitin sulphate (#1133570, lot #087K1416; Sigma-Aldrich, Merck, Darmstadt, Germany) as the reference standard.

#### Osteogenic Differentiation

ADSCs were cultured as monolayers at a density of  $5 \times 10^3$  cells/ $\text{cm}^2$  and differentiated using the STEMPRO Osteogenesis Differentiation Kit (A10069, lot #2216485; Gibco, Waltham, MA, USA) for three weeks. Calcium deposition was assessed by Von Kossa staining. Briefly, the cell monolayer was fixed in 10 % formaldehyde (F8775, lot #1359985; AppliChem, Darmstadt, Germany)/PBS for 5 minutes, washed with water, and incubated in 5 % silver nitrate (#131459, lot #MKBQ3322; AppliChem, Darmstadt, Germany) for 5 minutes. The monolayer was then exposed to ultraviolet light for 20 minutes, allowing the silver deposition to replace the reduced calcium. To remove unreacted silver, the cells were washed with 5 % sodium thiosulfate (#131721, lot #S67472; AppliChem, Darmstadt, Germany) and rinsed with distilled water afterwards.

#### Adipogenic Differentiation

ADSCs were cultured in monolayers at a density of  $2.5 \times 10^4$  cells/ $\text{cm}^2$  under two alternating culture conditions: Adipogenesis-maintenance medium (DMEM/Ham's F12 (#1-26F09-I, lot #SH09306P; Bioconcept, Allschwil, Switzerland), 2.5 % FBS, 1 $\times$  penicillin-streptomycin solution, 2.5  $\mu\text{g}/\text{mL}$  amphotericin B, and 170 mM insulin (I6634, lot #SLBL0827V; Sigma-Aldrich, Merck, Darmstadt, Germany)) and adipogenesis-inducing medium (adipogenesis maintenance medium supplemented with 1  $\mu\text{M}$  dexamethasone, 0.5 mM 3-Isobutyl-1-methylxanthine (I5879, lot #0001416650), and 0.2 mM indomethacin (I7378, lot #1353739); all from Sigma-Aldrich, Merck, Darmstadt, Germany). After two weeks of differentiation, the lipid droplets were stained with Oil Red O (O0625, lot #039k-1466; Sigma-Aldrich, Merck, Darmstadt, Germany).

For 3D cell culture, cryosections (20  $\mu\text{m}$ ) of the cell constructs were fixed in 10 % formaldehyde/PBS for 5 minutes. The slides were then washed with 60 % isopropyl alcohol (I9030, lot #9F011108; AppliChem, Darmstadt, Germany) for 5 minutes before being stained with filtered (0.2  $\mu\text{m}$ ) Oil Red O solution for 10 minutes. After staining, the slides were washed again with 60 % isopropyl alcohol for 2 minutes, followed by rinsing in distilled water. Finally, the slides were mounted with 70 % glycerol (A3739, lot #2217823; AppliChem, Darmstadt, Germany) and examined under a light microscope.



## Statistical Analysis

Differences between samples ( $n = 6$ ) were evaluated using the non-parametric Wilcoxon signed-rank test for dependent variables, with statistical significance defined as  $p < 0.05$ . The matched pairs rank biserial correlation coefficient ( $r_{rb}$ ) was used to measure the effect size, which represents the probability that a randomly selected pair will be in the predicted order. The categorisation for rank-biserial  $r_{rb}$  is considered “extremely strong” (perfect positive effect) between 0.9 to 1.0, “very strong” between 0.7 and 0.9 and “strong” between 0.5 and 0.7. Based on our sample size (6 matched pairs), a power of 80 %, and a two-sided alpha level of 0.05, the resulting detectable rank-biserial correlation was 0.81 (calculated with R package pROC (Version 1.19.0.01) used in RStudio software (Version 2025.05.1, Posit Team, Boston, MA, USA)). All data analyses were conducted using SPSS version 24.0 for Windows (IBM Corp., Armonk, CA, USA). Schematic representations and figures were generated using BioRender (<https://www.biorender.com/>).

## Results

### Characterization of Adipose-Derived Stromal Cells

Flow cytometry analysis confirmed that the isolated ADSCs expressed mesenchymal stem cell markers *CD44*, *CD90*, and *CD105*, while lacking the haematopoietic marker *CD14* (Fig. 1, top right). In addition, the multipotent nature of the isolated cells was verified through differentiation assays. Adipogenic differentiation was confirmed by lipid vacuole accumulation (Oil Red O staining), while osteogenic and chondrogenic differentiation were confirmed by Von Kossa staining for mineral deposition and glycosaminoglycan production ( $p < 0.01$ ,  $r_{rb} = -1$ ), respectively (Fig. 1, lower panels).

### Effects of Mechanical Processing on Stem Cell Yield and Senescence

Lipoaspirates (“Millifat”) were processed using the Lipocube system to yield distinct fat fractions: unprocessed “Microfat”, “emulsified Microfat”, and “Nanofat” (Fig. 2a). Quantitative analysis showed that highest ADSCs yield was obtained from unprocessed Microfat (26 % increase compared to Millifat) followed by emulsified Microfat (14 % increase compared to Millifat) and Nanofat (14 % reduction compared to Millifat; Fig. 2b). Although the reduction in yield did not reach statistical significance, mechanical processing notably decreased cell yield due to the loss of biological material. Cellular senescence, as measured by fluorometric analysis, decreased following mechanical processing. Specifically, compared with Millifat, senescence was reduced by 6 % in Microfat, 12 % in emulsified Microfat ( $p < 0.05$ ,  $r_{rb} = -1$ ), and 4 % in Nanofat.

### Impact of Platelet-Rich Plasma on ADSCs Cultures

The effects of different PRP concentrations (1 %, 5 %, and 10 %) on ADSCs monolayer cultures were evaluated over a 5-day period (Fig. 3). Compared to the positive control (medium supplemented with FGF), both the negative control (FBS only) and cultures with 1 % PRP showed a significant reduction in cell proliferation (40 %,  $r_{rb} = 1$  and 20 %,  $r_{rb} = 0.9$ , respectively;  $p < 0.05$ ), larger cell volume (35 % increase for both;  $p < 0.05$  and  $r_{rb} = -1$ ), and a substantial increase in cell senescence (70 %,  $r_{rb} = -1$  and 20 %,  $r_{rb} = -0.6$ , respectively;  $p < 0.05$ ). In contrast, supplementation with 5 % and 10 % PRP maintained proliferation, cell volume, and senescence levels comparable to those observed in FGF-supplemented cultures. Notably, 5 % PRP consistently enhanced these parameters, suggesting that this is the optimal concentration for supporting ADSCs cultures.

### Comparison of Scaffolds in Supporting Adipogenic Differentiation

Three collagen-based scaffolds (BioPad, FibroGide, and Suprasorb) were compared for their capacity to support adipogenic differentiation of ADSCs over 14 days period. Morphological assessment revealed that cell constructs on BioPad exhibited significant shrinkage (85 %), whereas those on Suprasorb (40 %) and FibroGide (5 %) showed a reduction and a minimal shrinkage respectively (Fig. 4a). Oil Red O staining confirmed the accumulation of lipid droplets in all scaffolds, indicating adipogenic differentiation (Fig. 4b). Moreover, quantitative PCR analysis of adipogenic markers (*FABP4*, *GLUT4*, and *LPL*) demonstrated higher expression levels in constructs using FibroGide and Suprasorb compared with BioPad and monolayer cultures (Fig. 4c).

### Endothelial Differentiation of ADSCs-HUVEC Co-Cultures

Co-culture experiments using ADSCs and HUVECs (8:2 ratio) on FibroGide scaffolds demonstrated that ADSCs supported endothelial differentiation. Gene expression analysis showed that cells cultured with growth factors (EBM-2 + growth factors (GF)) exhibited a 40 % reduction in *CD31* and a 48 % reduction in *VEGFR2* expression, with a marginal change in *vWF* expression (+5 %) compared to those cultured with EBM-2 + 2 % FBS (Fig. 5a). In cultures supplemented with 5 % PRP, *CD31* expression decreased by 41 % and *vWF* by 25 %, whereas *VEGFR2* remained nearly unchanged (−6 %). Immunohistochemical staining further confirmed the localisation of the endothelial markers *CD31*, *VEGFR2*, and *vWF* within the three-dimensional constructs (Fig. 5b).

### Characterization and Effects of ADSCs-Derived Exosomes

Nanoparticle tracking analysis of ADSC-derived exosomes revealed a predominant particle size of approxi-



mately 119 nm (Fig. 6a), which was confirmed by fluorescence microscopy (Fig. 6b). When ADSCs monolayers were cultured for five days with 10  $\mu\text{g/mL}$  exosomes, no significant changes in cell proliferation or volume were observed compared to the negative control (without FGF supplementation; Fig. 6c). However, compared to the FGF-supplemented control, ADSCs proliferation was significantly lower (2.3-fold to 1.3-fold,  $p < 0.01$  and  $r_{rb} = 1$ ), and cell volume was increased (0.9-fold to 1.0-fold,  $p < 0.05$  and  $r_{rb} = -0.82$ ). Notably, exosome treatment was associated with the upregulation of stem cell markers (Fig. 6c). Compared to the negative control, *CD90* expression in ADSCs cultured in FGF increased from 0.8-fold to 2.1-fold with exosomes, and *MCP-1* expression increased from 2.1-fold with FGF to 4.8-fold with exosomes, suggesting a role for exosomes in maintaining stemness in ADSCs.

## Discussion

Conventional wound care methods often fail to achieve complete PIs healing, resulting in prolonged recovery periods and repeated interventions. PIs reconstruction using a fasciocutaneous flap remains a significant clinical challenge due to the high risk of complications, such as infections, wound healing disorders and eventually ulcer recurrence [43]. The present study offers valuable insights into the development of a cell-based therapy for PIs treatment by combining autologous cells with biomaterials to enhance tissue repair.

Based on the results presented in this study, each component will be combined to generate a minimally invasive protocol for implementation during surgical reconstruction of PIs. In our approach, emulsified Microfat, PRP, and porous collagen scaffolds were tested for potential application to the PIs. Based on these results, our proposed translational method utilises a “sandwich” technique, whereby PRP is first applied to the wound bed, followed by a layer of collagen scaffold and a fasciocutaneous flap enriched with emulsified Microfat infiltration and exosomes. The combination of MSCs with biomaterials offers several advantages, including enhanced cell viability, targeted delivery, and improved retention of cells at the injury site. These factors will potentially contribute to increased angiogenesis [44], accelerated re-epithelialization [45], and overall enhanced tissue regeneration [46]. Furthermore, by utilising fresh autologous cells, our approach circumvents the potential drawbacks associated with extensive *ex vivo* expansion, such as the onset of cellular senescence [47]. Additionally, the use of FibroGide as a scaffold mitigates concerns regarding rapid degradation, as our results demonstrated minimal size reduction in culture. To overcome the logistical and regulatory challenges commonly associated with translating *in vitro* research into clinical applications, all biological materials employed are autologous (except for the scaffold and exosomes), obtained using clinically approved devices in compliance with Good Clinical Practice (GCP)

standards, and are readily available through minimally manipulated systems designed for the surgical theatre.

Cell-based therapies are already applied alongside standard wound care strategies, such as debridement, direct surgical closure, or reconstructive flap surgery, to expedite wound healing. Emerging evidence highlights the potential of ADSCs and MSCs in chronic wound healing, although their use in adult PIs has not been the primary focus [48]. ADSCs-based interventions have been shown to enhance angiogenesis, accelerate re-epithelialisation, improve granulation tissue formation, and promote faster wound closure [49]. For example, autologous MSC therapy for diabetic foot ulcers led to a 72 % reduction in ulcer size and improved pain-free walking [50]. Currently, MSCs are being employed in a phase I/II, multicentre, randomised, controlled clinical trial to provide an effective treatment for venous leg ulcers, potentially reducing wound closure time and associated complications [51]. Additionally, a study utilising MSC-seeded collagen sponges as wound dressings in patients with intractable dermatopathies reported complete wound healing in 18 of 20 patients [52].

Fat grafts also play a crucial role in tissue engineering because of their high content of growth factors and ADSCs, as well as their ease of harvest, safety, and cost-effectiveness [53]. Fat grafting, an autologous tissue transfer technique, offers advantages such as natural integration into host tissues and potential long-term volume retention. Advances in fat grafting, particularly the use of injectable emulsified fat obtained through lipoaspirate emulsification and filtration, have led to improved graft survival [16]. A recent study has also suggested a synergistic effect between fat tissue and PRP in promoting tissue regeneration and accelerating recovery [54].

PRP, derived from centrifuged whole blood, provides a concentrated solution of alpha granules rich in growth factors [55]. When combined with fat grafts, PRP significantly enhances fat cell survival by promoting cell proliferation [56], and its bioactive components accelerate wound healing [57]. PRP also exhibits anti-inflammatory properties and reduces fat necrosis and cell death, reinforcing its role in adipose tissue regeneration [53]. In contrast, ADSCs-derived exosomes did not modify ADSCs proliferation but promoted the maintenance of stemness, as evidenced by the increased expression of *CD90* and *MCP-1*, compared to standard culture conditions supplemented with FGF. The preservation of stemness and the presence of stem cells influence the efficacy and quality of wound healing, both through direct cellular contributions and extensive paracrine immuno-modulation of the wound microenvironment. These observations imply that PRP and exosomes may have complementary roles: PRP supports host tissue regrowth, whereas exosomes prolong ADSCs longevity *in situ*. In addition, MSC-derived exosomes have been shown to significantly induce the proliferation and migration of key skin cells [26], such as dermal fibroblasts and ker-

atinocytes, which are crucial players in re-epithelialisation and the formation of new tissue, by increasing the phosphorylation of extracellular signal-regulated kinase (ERK)-1/2 [58] or by activating signalling pathways such as Wnt/ $\beta$ -catenin and Akt [59]. Consequently, the combined application of PRP and exosomes holds significant promise for enhanced wound healing in the proposed cell-based therapy for PIs.

We also assessed various scaffolds to establish a protocol to ensure the survival of ADSCs after flap reconstruction of PIs. Among the tested matrices, FibroGide and Suprasorb exhibited excellent handling characteristics and efficiently absorbed the cell suspension without leaving residual cells in the culture plate. Notably, FibroGide and, to a lesser extent, Suprasorb, maintained their structural integrity during cell culture, making them suitable for withstanding local body pressure. Histological analysis confirmed fat deposition throughout the scaffolds, reinforcing their potential as biomaterials for ADSCs therapy in regenerative medicine. Additionally, co-culture experiments employing HUVECs as a proxy for blood vessel formation demonstrated that ADSCs contributed to early vascular network formation in a three-dimensional environment. This finding suggests that implanting an ADSCs-scaffold construct may improve wound healing by supporting vascularisation and tissue regeneration, thereby contributing to the establishment of a stable microvascular network [60].

Despite these promising findings, several limitations warrant further consideration. First, the *in vitro* model may not fully replicate the complexity of the wound microenvironment, potentially affecting the translation of the results to clinical applications. Nevertheless, our method was specifically designed to reduce key translational risks, including immunogenicity and long-term safety. The use of autologous cells and natural biomaterials, such as collagen, a biodegradable and biocompatible polymer, minimises the risk of immune rejection due to their inherently low antigenicity. Furthermore, current clinical trials involving MSCs have not reported tumorigenic complications, supporting their safety profiles for regenerative applications [49]. To further mitigate the potential risk of cellular transformation and reduce manufacturing costs, our approach avoids *ex vivo* expansion of ADSCs, relying instead on fresh, minimally manipulated autologous material. Second, one of the major challenges in wound healing research is to validate laboratory data by finding good animal models which mirror the human condition. Animal models must fulfil the requirements associated with the basic biochemistry, physiology, and general biology of PIs, which can be achieved using an ischaemia-reperfusion model in mice and rats [61]. Unfortunately, the use of animal models for PIs presents several challenges related to anatomy (mice and rats have higher hair density and thinner skin than humans), the immune system (immune and inflammatory responses are significantly different from those in hu-

mans), and ethical considerations (due to stringent guidelines and ethical concerns) [62]. These factors collectively underscore the difficulty of accurately modelling human PIs in animals and highlight the need to apply alternatives before requesting animal licences. Recent advances in human micro-physiological systems now enable direct investigation of chronic wound biology without the use of animals. By demonstrating clinically relevant endpoints, such as reduced ADSC senescence, optimised PRP dosing, and early angiogenic responses, our approach not only fulfils ethical considerations but also provides robust quantitative benchmarks for future translational or *in vivo* investigations. Therefore, in this study, we opted for a different approach based on *in vitro* and controlled conditions. However, diverse animal studies have already shown the beneficial impact of implementing ADSCs [63], PRP [13,64], and ADSCs-derived exosomes [65] during flap reconstruction. Third, autologous PRP can exhibit variability in efficacy owing to differences in preparation methods, leading to inconsistent growth factor content and reproducibility challenges [66]. Lastly, while we acknowledge the limitations of a small sample size, the focus of this study was on assessing cellular responses under controlled conditions rather than achieving a statistical representation of the broader population. In our study, most comparisons yielded a rank-biserial correlation greater than 0.8 or lower than -0.8, indicating that the sample size was sufficient. Only male patients were included, initially because the study also aimed to investigate the potential influence of testosterone on ADSCs. Although this part of the project was discontinued due to inconclusive results, the donor pool remained restricted to men. This choice reduces biological variability in our experiments and reflects the predominance of male individuals with SCI in our clinic, but we acknowledge that it limits the generalizability of our findings. Indeed, future research should focus on clinical validation to assess long-term outcomes, refine therapeutic protocols, broaden the patient pool, and standardise PRP-based applications for the treatment of PIs.

## Conclusions

This study established an *in vitro* foundation for a minimally manipulated, autologous cell-based approach aimed at improving wound healing in PIs among patients with SCI. Mechanically derived ADSCs, PRP, and collagen scaffolds promoted adipogenic differentiation, reduced cellular senescence, and supported early vascularisation under controlled conditions. The proposed sandwich technique—which involves applying PRP to the wound bed, placing a collagen scaffold (FibroGide or Suprasorb), and enhancing with emulsified Microfat infiltration—may represent a feasible and reproducible protocol for accelerating tissue repair following reconstructive surgery. While each component appears to contribute beneficially to cellular and molecular parameters relevant to wound healing, the

*in vitro* model employed does not fully capture the complexity of the wound microenvironment *in vivo*. Therefore, these findings should be interpreted as preliminary and warrant further validation through comprehensive *in vivo* and clinical trials. Nevertheless, the findings and developments described set the foundation for future interventions aimed at accelerating healing in patients with SCI after surgical PIs reconstruction.

## List of Abbreviations

PIs, pressure injuries; SCI, spinal cord injury; ADSCs, adipose-derived stromal cells; PRP, platelet-rich plasma; HUVECs, human umbilical vein endothelial cells; MSCs, mesenchymal stem cells; PDGF, platelet-derived growth factor; VEGF, vascular endothelial growth factor; TGF- $\beta$ , transforming growth factor- $\beta$ ; IGF, insulin-like growth factor; EGF, epidermal growth factor; GAG, glycosaminoglycan;  $r_{rb}$ , matched pairs rank biserial correlation coefficient; *vWF*, von Willebrand factor; GCP, Good Clinical Practice; ERK, extracellular signal-regulated kinase; RT, room temperature; 3D, three-dimensional; PBS, phosphate-buffered saline; FBS, foetal bovine serum; FITC, fluorescein isothiocyanate; *CD14*, cluster of differentiation 14; FGF, fibroblast growth factor; SEM, standard error of the mean; qPCR, quantitative polymerase chain reaction; BSA, bovine serum albumin; GF, growth factors; *FABP4*, fatty acid binding protein 4; *GLUT4*, glucose transporter type 4; *LPL*, lipoprotein lipase; *GAPDH*, glyceraldehyde 3-phosphate dehydrogenase; *VEGFR-2*, vascular endothelial growth factor receptor 2; EGM-2, endothelial cell growth medium 2; cDNA, complementary DNA; DMEM, Dulbecco's Modified Eagle Medium; EBM-2, endothelial basal medium-2.

## Availability of Data and Materials

Not Applicable.

## Author Contributions

AB, RW and JS conceptualized the project. RW, JB, AH and NS were involved in the recruitment of patients and collection of samples. AB, NN, SSo and SSa conducted the laboratory analyses and analysed the data. AB conducted the statistical analysis. AB and JS wrote the main manuscript. All authors have reviewed and approved the final manuscript.

## Ethics Approval and Consent to Participate

This study was approved by the Ethics Committee of Northwest and Central Switzerland (project ID: 2019-01062), in accordance with the Declaration of Helsinki. Written informed consent was obtained from all the participants.

## Acknowledgments

We thank the participants for their participation in the study and acknowledge the support of the field staff in sample collection at the Swiss Paraplegic Centre, Nottwil, Switzerland. We thank Dr. Ali Hashemi at the University of Bern for contributing to exosome characterisation.

## Funding

This research was supported by the Swiss Paraplegic Foundation (Grant: Foko\_2018\_03) and the Swiss Paraplegic Research.

## Conflict of Interest

The authors declare that they have no competing interests.

## References

- [1] Gélis A, Dupeyron A, Legros P, Benaïm C, Pelissier J, Fattal C. Pressure ulcer risk factors in persons with spinal cord injury part 2: the chronic stage. *Spinal Cord*. 2009; 47: 651–661. <https://doi.org/10.1038/sc.2009.32>.
- [2] Rappl LM. Physiological changes in tissues denervated by spinal cord injury tissues and possible effects on wound healing. *International Wound Journal*. 2008; 5: 435–444. <https://doi.org/10.1111/j.1742-481X.2007.00360.x>.
- [3] Scheel-Sailer A, Wyss A, Boldt C, Post MW, Lay V. Prevalence, location, grade of pressure ulcers and association with specific patient characteristics in adult spinal cord injury patients during the hospital stay: a prospective cohort study. *Spinal Cord*. 2013; 51: 828–833. <https://doi.org/10.1038/sc.2013.91>.
- [4] Najmanova K, Neuhauser C, Krebs J, Baumberger M, Schaefer DJ, Sailer CO, *et al.* Risk factors for hospital acquired pressure injury in patients with spinal cord injury during first rehabilitation: prospective cohort study. *Spinal Cord*. 2022; 60: 45–52. <https://doi.org/10.1038/s41393-021-00681-x>.
- [5] DeVivo MJ, Farris V. Causes and Costs of Unplanned Hospitalizations Among Persons with Spinal Cord Injury. *Topics in Spinal Cord Injury Rehabilitation*. 2011; 16: 53–61. <https://doi.org/10.1310/sci1604-53>.
- [6] Edlich RF, Winters KL, Woodard CR, Buschbacher RM, Long WB, Gebhart JH, *et al.* Pressure ulcer prevention. *Journal of Long-Term Effects of Medical Implants*. 2004; 14: 285–304. <https://doi.org/10.1615/jlongtermeffmedimplants.v14.i4.20>.
- [7] Wettstein R, Tremp M, Baumberger M, Schaefer DJ, Kalbermatten DF. Local flap therapy for the treatment of pressure sore wounds. *International Wound Journal*. 2015; 12: 572–576. <https://doi.org/10.1111/iwj.12166>.
- [8] Frazier T, Alarcon A, Wu X, Mohiuddin OA, Motherwell JM, Carlsson AH, *et al.* Clinical Translational Potential in Skin Wound Regeneration for Adipose-Derived, Blood-Derived, and Cellulose Materials: Cells, Exosomes, and Hydrogels. *Biomolecules*. 2020; 10: 1373. <https://doi.org/10.3390/biom10101373>.
- [9] Mazini L, Rochette L, Admou B, Amal S, Malka G. Hopes and Limits of Adipose-Derived Stem Cells (ADSCs) and Mesenchymal Stem Cells (MSCs) in Wound Healing. *International Journal of Molecular Sciences*. 2020; 21: 1306. <https://doi.org/10.3390/ijms21041306>.
- [10] Ferraro GA, De Francesco F, Nicoletti G, Paino F, Desiderio V, Tirino V, *et al.* Human adipose CD34<sup>+</sup> CD90<sup>+</sup> stem cells and collagen scaffold constructs grafted *in vivo* fabricate loose connective and adipose tissues. *Journal of Cellular Biochemistry*. 2013; 114: 1039–1049. <https://doi.org/10.1002/jcb.24443>.
- [11] Trzyna A, Banaś-Ząbczyk A. Adipose-Derived Stem Cells Se-



- cretome and Its Potential Application in “Stem Cell-Free Therapy”. *Biomolecules*. 2021; 11: 878. <https://doi.org/10.3390/biom11060878>.
- [12] Cao Y, Sun Z, Liao L, Meng Y, Han Q, Zhao RC. Human adipose tissue-derived stem cells differentiate into endothelial cells *in vitro* and improve postnatal neovascularization *in vivo*. *Biochemical and Biophysical Research Communications*. 2005; 332: 370–379. <https://doi.org/10.1016/j.bbrc.2005.04.135>.
  - [13] Smith OJ, Jell G, Mosahebi A. The use of fat grafting and platelet-rich plasma for wound healing: A review of the current evidence. *International Wound Journal*. 2019; 16: 275–285. <https://doi.org/10.1111/iwj.13029>.
  - [14] Cohen SR, Womack H, Ghanem A. Fat Grafting for Facial Rejuvenation through Injectable Tissue Replacement and Regeneration: A Differential, Standardized, Anatomic Approach. *Clinics in Plastic Surgery*. 2020; 47: 31–41. <https://doi.org/10.1016/j.cps.2019.08.005>.
  - [15] Coleman SR. Structural fat grafting: more than a permanent filler. *Plastic and Reconstructive Surgery*. 2006; 118: 108S–120S. <https://doi.org/10.1097/01.prs.0000234610.81672.e7>.
  - [16] Tonnard P, Verpaele A, Peeters G, Hamdi M, Cornelissen M, Declercq H. Nanofat grafting: basic research and clinical applications. *Plastic and Reconstructive Surgery*. 2013; 132: 1017–1026. <https://doi.org/10.1097/PRS.0b013e31829fe1b0>.
  - [17] Huang S, Li Q, Li X, Ye H, Zhang L, Zhu X. Recent Research Progress of Wound Healing Biomaterials Containing Platelet-Rich Plasma. *International Journal of Nanomedicine*. 2025; 20: 3961–3976. <https://doi.org/10.2147/IJN.S506677>.
  - [18] Xu H, Huang K, Tao X. Efficacy and safety of platelet-rich plasma versus conventional care in diabetic foot ulcers: a meta-analysis of randomized controlled trials. *Acta Diabetologica*. 2025. (online ahead of print) <https://doi.org/10.1007/s00592-025-02555-7>.
  - [19] Marx RE. Platelet-rich plasma: evidence to support its use. *Journal of Oral and Maxillofacial Surgery: Official Journal of the American Association of Oral and Maxillofacial Surgeons*. 2004; 62: 489–496. <https://doi.org/10.1016/j.joms.2003.12.003>.
  - [20] Kang YH, Jeon SH, Park JY, Chung JH, Choung YH, Choung HW, *et al.* Platelet-rich fibrin is a Bioscaffold and reservoir of growth factors for tissue regeneration. *Tissue Engineering. Part A*. 2011; 17: 349–359. <https://doi.org/10.1089/ten.TEA.2010.0327>.
  - [21] Sun Y, Zhu M, Qiu L. Efficacy of mesenchymal stem cells and platelet-rich plasma therapies on wound healing: A Systematic Review and meta-analysis. *Regenerative Therapy*. 2025; 30: 75–91. <https://doi.org/10.1016/j.reth.2025.04.010>.
  - [22] Feng H, Gong S, Liu Y, Aghayants S, Liu Y, Wu M, *et al.* Adipose-derived stem cell exosomes: mechanisms and therapeutic potentials in wound healing. *Biomarker Research*. 2025; 13: 88. <https://doi.org/10.1186/s40364-025-00801-2>.
  - [23] Pan W, Chen H, Wang A, Wang F, Zhang X. Challenges and strategies: Scalable and efficient production of mesenchymal stem cells-derived exosomes for cell-free therapy. *Life Sciences*. 2023; 319: 121524. <https://doi.org/10.1016/j.lfs.2023.121524>.
  - [24] Ha DH, Kim HK, Lee J, Kwon HH, Park GH, Yang SH, *et al.* Mesenchymal Stem/Stromal Cell-Derived Exosomes for Immunomodulatory Therapeutics and Skin Regeneration. *Cells*. 2020; 9: 1157. <https://doi.org/10.3390/cells9051157>.
  - [25] An Y, Lin S, Tan X, Zhu S, Nie F, Zhen Y, *et al.* Exosomes from adipose-derived stem cells and application to skin wound healing. *Cell Proliferation*. 2021; 54: e12993. <https://doi.org/10.1111/cpr.12993>.
  - [26] Hu L, Wang J, Zhou X, Xiong Z, Zhao J, Yu R, *et al.* Exosomes derived from human adipose mesenchymal stem cells accelerates cutaneous wound healing via optimizing the characteristics of fibroblasts. *Scientific Reports*. 2016; 6: 32993. <https://doi.org/10.1038/sr32993>.
  - [27] Seth G, Singh S, Sharma G, Suvedi D, Kumar D, Nagraik R, *et al.* Harnessing the power of stem cell-derived exosomes: a rejuvenating therapeutic for skin and regenerative medicine. *3 Biotech*. 2025; 15: 184. <https://doi.org/10.1007/s13205-025-04345-y>.
  - [28] Yang G, Waheed S, Wang C, Shekh M, Li Z, Wu J. Exosomes and Their Bioengineering Strategies in the Cutaneous Wound Healing and Related Complications: Current Knowledge and Future Perspectives. *International Journal of Biological Sciences*. 2023; 19: 1430–1454. <https://doi.org/10.7150/ijbs.80430>.
  - [29] Ratcliffe A, Butler DL, Dymont NA, Cagle PJ Jr, Proctor CS, Ratcliffe SS, *et al.* Scaffolds for tendon and ligament repair and regeneration. *Annals of Biomedical Engineering*. 2015; 43: 819–831. <https://doi.org/10.1007/s10439-015-1263-1>.
  - [30] Munir N, Callanan A. Novel phase separated polycaprolactone/collagen scaffolds for cartilage tissue engineering. *Biomedical Materials*. 2018; 13: 051001. <https://doi.org/10.1088/1748-605X/aac91f>.
  - [31] Wang X, Wu P, Hu X, You C, Guo R, Shi H, *et al.* Polyurethane membrane/knitted mesh-reinforced collagen-chitosan bilayer dermal substitute for the repair of full-thickness skin defects via a two-step procedure. *Journal of the Mechanical Behavior of Biomedical Materials*. 2016; 56: 120–133. <https://doi.org/10.1016/j.jmbbm.2015.11.021>.
  - [32] World Medical Association. World Medical Association Declaration of Helsinki: Ethical Principles for Medical Research Involving Human Participants. *JAMA*. 2025; 333: 71–74. <https://doi.org/10.1001/jama.2024.21972>.
  - [33] Tiryaki KT, Cohen S, Kocak P, Canikyan Turkey S, Hewett S. *In-Vitro* Comparative Examination of the Effect of Stromal Vascular Fraction Isolated by Mechanical and Enzymatic Methods on Wound Healing. *Aesthetic Surgery Journal/the American Society for Aesthetic Plastic Surgery*. 2020; 40: 1232–1240. <https://doi.org/10.1093/asj/sjaa154>.
  - [34] Güven S, Mehrkens A, Saxer F, Schaefer DJ, Martinetti R, Martin I, *et al.* Engineering of large osteogenic grafts with rapid engraftment capacity using mesenchymal and endothelial progenitors from human adipose tissue. *Biomaterials*. 2011; 32: 5801–5809. <https://doi.org/10.1016/j.biomaterials.2011.04.064>.
  - [35] Bertolo A, Baur M, Guerrero J, Pötzel T, Stoyanov J. Autofluorescence is a Reliable *in vitro* Marker of Cellular Senescence in Human Mesenchymal Stromal Cells. *Scientific Reports*. 2019; 9: 2074. <https://doi.org/10.1038/s41598-019-38546-2>.
  - [36] Shin KO, Ha DH, Kim JO, Crumrine DA, Meyer JM, Wakefield JS, *et al.* Exosomes from Human Adipose Tissue-Derived Mesenchymal Stem Cells Promote Epidermal Barrier Repair by Inducing de Novo Synthesis of Ceramides in Atopic Dermatitis. *Cells*. 2020; 9: 680. <https://doi.org/10.3390/cells9030680>.
  - [37] Cho BS, Kim JO, Ha DH, Yi YW. Exosomes derived from human adipose tissue-derived mesenchymal stem cells alleviate atopic dermatitis. *Stem Cell Research & Therapy*. 2018; 9: 187. <https://doi.org/10.1186/s13287-018-0939-5>.
  - [38] Ha DH, Kim SD, Lee J, Kwon HH, Park GH, Yang SH, *et al.* Toxicological evaluation of exosomes derived from human adipose tissue-derived mesenchymal stem/stromal cells. *Regulatory Toxicology and Pharmacology: RTP*. 2020; 115: 104686. <https://doi.org/10.1016/j.yrtph.2020.104686>.
  - [39] Ambrosio L, Schol J, Ruiz-Fernandez C, Tamagawa S, Soma H, Tilotta V, *et al.* ISSLS PRIZE in Basic Science 2024: superiority of nucleus pulposus cell- versus mesenchymal stromal cell-derived extracellular vesicles in attenuating disc degeneration and alleviating pain. *European Spine Journal: Official Publication of the European Spine Society, the European Spinal Deformity Society, and the European Section of the Cervical Spine Research Society*. 2024; 33: 1713–1727. <https://doi.org/10.1007/s00586-024-08163-3>.
  - [40] Su X, Yao X, Sun Z, Han Q, Zhao RC. Optimization of Reference Genes for Normalization of Reverse Transcription Quantitative Real-Time Polymerase Chain Reaction Results in Senescence Study of Mesenchymal Stem Cells. *Stem Cells and Development*. 2016;



- 25: 1355–1365. <https://doi.org/10.1089/scd.2016.0031>.
- [41] Bertolo A, Mehr M, Aebli N, Baur M, Ferguson SJ, Stoyanov JV. Influence of different commercial scaffolds on the *in vitro* differentiation of human mesenchymal stem cells to nucleus pulposus-like cells. *European Spine Journal: Official Publication of the European Spine Society, the European Spinal Deformity Society, and the European Section of the Cervical Spine Research Society*. 2012; 2: S826–S838. <https://doi.org/10.1007/s00586-011-1975-3>.
- [42] Björnsson S. Simultaneous preparation and quantitation of proteoglycans by precipitation with alcian blue. *Analytical Biochemistry*. 1993; 210: 282–291. <https://doi.org/10.1006/abio.1993.1197>.
- [43] Chiu YJ, Liao WC, Wang TH, Shih YC, Ma H, Lin CH, *et al.* A retrospective study: Multivariate logistic regression analysis of the outcomes after pressure sores reconstruction with fasciocutaneous, myocutaneous, and perforator flaps. *Journal of Plastic, Reconstructive & Aesthetic Surgery: JPRAS*. 2017; 70: 1038–1043. <https://doi.org/10.1016/j.bjps.2017.04.004>.
- [44] O'Loughlin A, Kulkarni M, Creane M, Vaughan EE, Mooney E, Shaw G, *et al.* Topical administration of allogeneic mesenchymal stromal cells seeded in a collagen scaffold augments wound healing and increases angiogenesis in the diabetic rabbit ulcer. *Diabetes*. 2013; 62: 2588–2594. <https://doi.org/10.2337/db12-1822>.
- [45] Navone SE, Pascucci L, Dossena M, Ferri A, Invernici G, Acerbi F, *et al.* Decellularized silk fibroin scaffold primed with adipose mesenchymal stromal cells improves wound healing in diabetic mice. *Stem Cell Research & Therapy*. 2014; 5: 7. <https://doi.org/10.1186/scrt396>.
- [46] Ribeiro J, Pereira T, Amorim I, Caseiro AR, Lopes MA, Lima J, *et al.* Cell therapy with human MSCs isolated from the umbilical cord Wharton jelly associated to a PVA membrane in the treatment of chronic skin wounds. *International Journal of Medical Sciences*. 2014; 11: 979–987. <https://doi.org/10.7150/ijms.9139>.
- [47] Bertolo A, Mehr M, Janner-Jametti T, Graumann U, Aebli N, Baur M, *et al.* An *in vitro* expansion score for tissue-engineering applications with human bone marrow-derived mesenchymal stem cells. *Journal of Tissue Engineering and Regenerative Medicine*. 2016; 10: 149–161. <https://doi.org/10.1002/term.1734>.
- [48] Camesi A, Wettstein R, Valido E, Nyfeler N, Stojic S, Glisic M, *et al.* Advancements in cell-based therapies for the treatment of pressure injuries: A systematic review of interventional studies. *Journal of Tissue Engineering*. 2023; 14: 20417314231201071. <https://doi.org/10.1177/20417314231201071>.
- [49] Huang YZ, Gou M, Da LC, Zhang WQ, Xie HQ. Mesenchymal Stem Cells for Chronic Wound Healing: Current Status of Preclinical and Clinical Studies. *Tissue Engineering. Part B, Reviews*. 2020; 26: 555–570. <https://doi.org/10.1089/ten.TEB.2019.0351>.
- [50] Dash NR, Dash SN, Routray P, Mohapatra S, Mohapatra PC. Targeting nonhealing ulcers of lower extremity in human through autologous bone marrow-derived mesenchymal stem cells. *Rejuvenation Research*. 2009; 12: 359–366. <https://doi.org/10.1089/rej.2009.0872>.
- [51] Costela-Ruiz VJ, González-Vigil E, Espinosa-Ibáñez O, Alcázar-Caballero RM, Melguizo-Rodríguez L, Fernández-López O, *et al.* Application of allogeneic adult mesenchymal stem cells in the treatment of venous ulcers: A phase I/II randomized controlled trial protocol. *PloS One*. 2025; 20: e0323173. <https://doi.org/10.1371/journal.pone.0323173>.
- [52] Yoshikawa T, Mitsuno H, Nonaka I, Sen Y, Kawanishi K, Inada Y, *et al.* Wound therapy by marrow mesenchymal cell transplantation. *Plastic and Reconstructive Surgery*. 2008; 121: 860–877. <https://doi.org/10.1097/01.prs.0000299922.96006.24>.
- [53] Smith OJ, Kanapathy M, Khajuria A, Prokopenko M, Hachach-Haram N, Mann H, *et al.* Protocol for a systematic review of the efficacy of fat grafting and platelet-rich plasma for wound healing. *Systematic Reviews*. 2017; 6: 111. <https://doi.org/10.1186/s13643-017-0505-8>.
- [54] Debuc B, Gendron N, Cras A, Rancic J, Philippe A, Cetrulo CL Jr, *et al.* Improving Autologous Fat Grafting in Regenerative Surgery through Stem Cell-Assisted Lipotransfer. *Stem Cell Reviews and Reports*. 2023; 19: 1726–1754. <https://doi.org/10.1007/s12015-023-10568-4>.
- [55] Pallua N, Pulsfort AK, Suschek C, Wolter TP. Content of the growth factors bFGF, IGF-1, VEGF, and PDGF-BB in freshly harvested lipoaspirate after centrifugation and incubation. *Plastic and Reconstructive Surgery*. 2009; 123: 826–833. <https://doi.org/10.1097/PRS.0b013e318199ef31>.
- [56] Atashi F, Jaconi ME, Pittet-Cuénod B, Modarressi A. Autologous platelet-rich plasma: a biological supplement to enhance adipose-derived mesenchymal stem cell expansion. *Tissue Engineering. Part C, Methods*. 2015; 21: 253–262. <https://doi.org/10.1089/ten.TEC.2014.0206>.
- [57] Cervelli V, Gentile P, Grimaldi M. Regenerative surgery: use of fat grafting combined with platelet-rich plasma for chronic lower-extremity ulcers. *Aesthetic Plastic Surgery*. 2009; 33: 340–345. <https://doi.org/10.1007/s00266-008-9302-z>.
- [58] Kim S, Lee SK, Kim H, Kim TM. Exosomes Secreted from Induced Pluripotent Stem Cell-Derived Mesenchymal Stem Cells Accelerate Skin Cell Proliferation. *International Journal of Molecular Sciences*. 2018; 19: 3119. <https://doi.org/10.3390/ijms19103119>.
- [59] Zhang B, Wang M, Gong A, Zhang X, Wu X, Zhu Y, *et al.* HucMSC-Exosome Mediated-Wnt4 Signaling Is Required for Cutaneous Wound Healing. *Stem Cells*. 2015; 33: 2158–2168. <https://doi.org/10.1002/stem.1771>.
- [60] Cao Y, Yan J, Dong Z, Wang J, Jiang X, Cui T, *et al.* Adipose-derived Mesenchymal Stem Cells are Ideal for the Cell-based Treatment of Refractory Wounds: Strong Potential for Angiogenesis. *Stem Cell Reviews and Reports*. 2024; 20: 313–328. <https://doi.org/10.1007/s12015-023-10641-y>.
- [61] Salcido R, Popescu A, Ahn C. Animal models in pressure ulcer research. *The Journal of Spinal Cord Medicine*. 2007; 30: 107–116. <https://doi.org/10.1080/10790268.2007.11753921>.
- [62] Kesarwani A, Nagpal PS, Chhabra HS. Experimental animal modelling for pressure injury: A systematic review. *Journal of Clinical Orthopaedics and Trauma*. 2021; 17: 273–279. <https://doi.org/10.1016/j.jcot.2021.04.001>.
- [63] Avila FR, Torres-Guzman RA, Huayllani MT, Guliyeva G, Zubair AC, Quiñones-Hinojosa A, *et al.* Human stem cells prevent flap necrosis in preclinical animal models: A systematic review. *Journal of Clinical and Translational Research*. 2022; 8: 110–124.
- [64] Sommeling CE, Heyneman A, Hoeksema H, Verbelen J, Stillaert FB, Monstrey S. The use of platelet-rich plasma in plastic surgery: a systematic review. *Journal of Plastic, Reconstructive & Aesthetic Surgery: JPRAS*. 2013; 66: 301–311. <https://doi.org/10.1016/j.bjps.2012.11.009>.
- [65] Mayo JS, Kurata WE, O'Connor KM, Pierce LM. Oxidative Stress Alters Angiogenic and Antimicrobial Content of Extracellular Vesicles and Improves Flap Survival. *Plastic and Reconstructive Surgery*. 2019; 7: e2588. <https://doi.org/10.1097/GOX.0000000000002588>.
- [66] Chattrathikul V, Pinthonglor P, Supanchart C, Sangin S. A comparative study of three liquid platelet concentrates on human primary osteoblast activity: an *in vitro* study. *Journal of Applied Oral Science: Revista FOB*. 2025; 33: e20240575. <https://doi.org/10.1590/1678-7757-2024-0575>.

**Editor's note:** The Scientific Editor responsible for this paper was Bo Lei.

**Received:** 10th March 2025; **Accepted:** 12th September 2025; **Published:** 28th November 2025